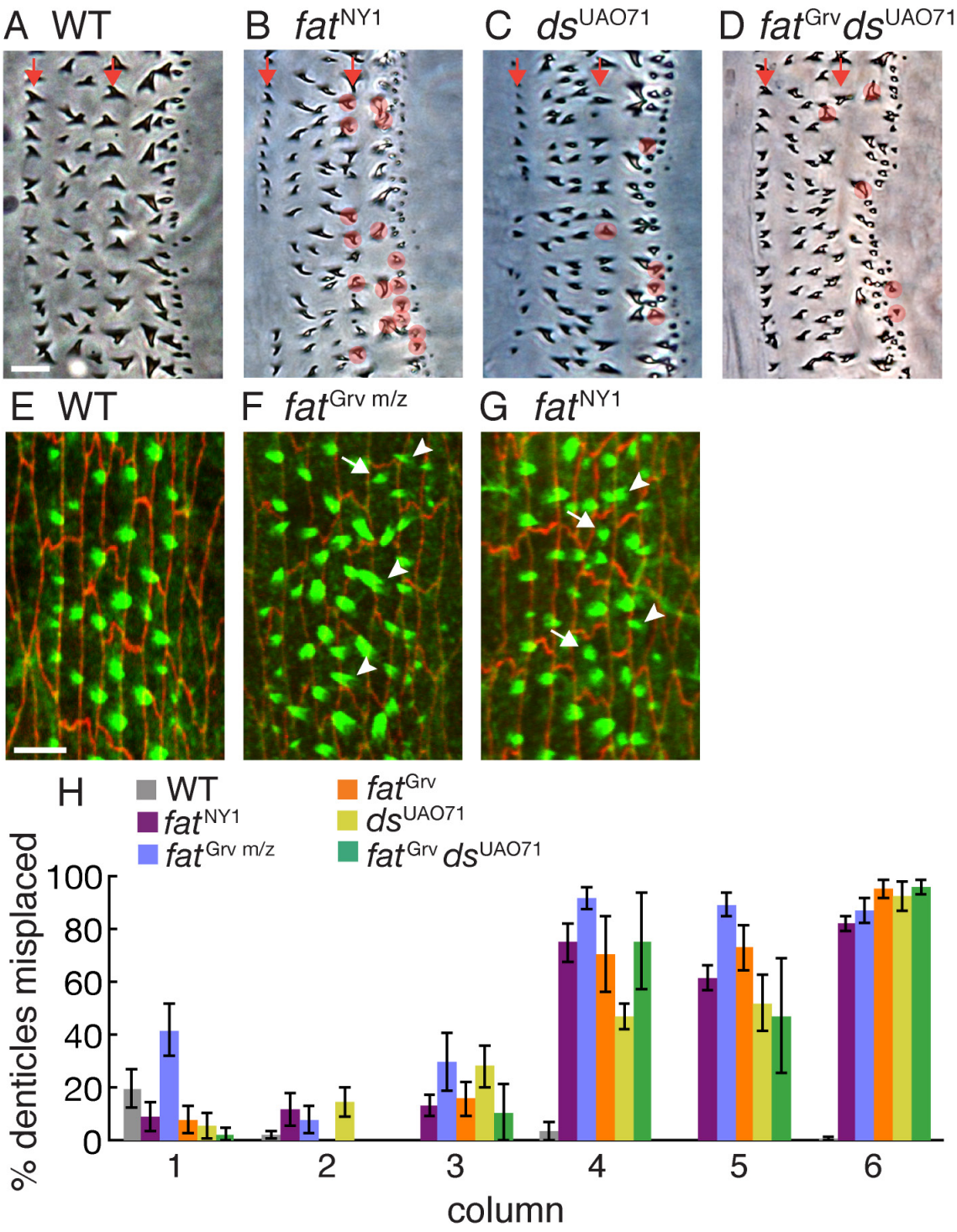

Fig. S1. Denticle placement defects in *fat* and *dachsous* mutants. (**A-D**) Cuticle preparations of wild-type (WT) (A), *fat*^{NY1} (B), *ds*^{UAO71} (C) and *fat*^{Grv} *ds*^{UAO71} (D) embryos. A majority of denticles point posteriorly in WT, with the exception of columns 1 and 4 (arrows), which point anteriorly. Misoriented denticles are highlighted in red. (**E-G**) Stage 15 denticle belts stained for F-actin (phalloidin, green) and E-cadherin (red) in WT (E), *fat*$^{Grv\ m/z}$ mutants that lack maternal and zygotic *fat* activity (F) and *fat*^{NY1} zygotic mutants (G). Ventral views, anterior left. (**H**) Percentage of misplaced denticle precursors by column in WT, *fat*^{NY1} zygotic mutants, *fat*$^{Grv\ m/z}$ mutants, *fat*^{Grv} zygotic mutants, *ds*^{UA071} zygotic mutants and *fat*^{Grv} *ds*^{UA071} double zygotic mutants. All mutants were significantly different from WT in columns 4-6 (P<0.01). All mutant genotypes except *fat*^{Grv} *ds*^{UA071} were significantly different from WT in column 3 (P<0.05). Denticle placement defects in embryos lacking maternal and zygotic *fat*^{Grv} activity were not significantly different from *fat*^{Grv} zygotic mutants except in column 1 (P=0.008). A single value was obtained for each column in each embryo (400-640 denticles in four to six embryos/genotype). The mean±s.e.m. of these values is shown. Scale bars: 5 μm.

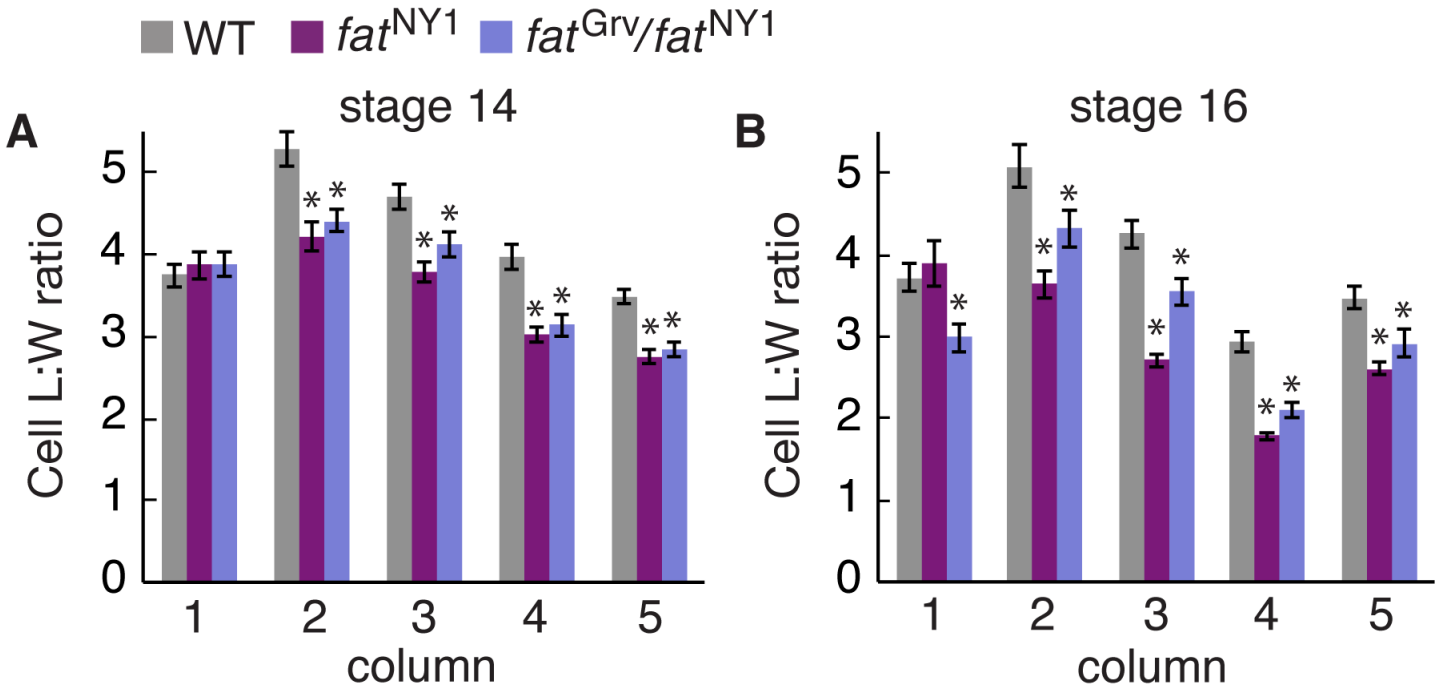

Fig. S2. Cell shape defects in *fat* mutants. Cell length:width (L:W) ratios (the ratio of cell length along the DV axis to cell width along the AP axis) plotted by column in stage 14 wild type (WT), *fat*^{NY1} zygotic mutant and *fat*^{Grv}/*fat*^{NY1} transheterozygous embryos. (**A**) Stage 14 cell L:W ratios were decreased in *fat*^{NY1} in columns 2-5 (P<0.001), and in *fat*^{Grv}/*fat*^{NY1} in columns 2 (P<0.001), 3 (P=0.01), 4 (P<0.001) and 5 (P<0.001). (**B**) Stage 16 cell L:W ratios were decreased in *fat*^{NY1} in columns 2-5 (P<0.001) and in *fat*^{Grv}/*fat*^{NY1} in columns 1 (P<0.01), 2(P<0.05), 3 (P<0.01), 4 (P<0.001) and 5 (P=0.012). A ratio was measured for each cell (40-75 cells in four embryos/column). The mean±s.e.m. of these values is shown. Asterisks indicate statistical significance.

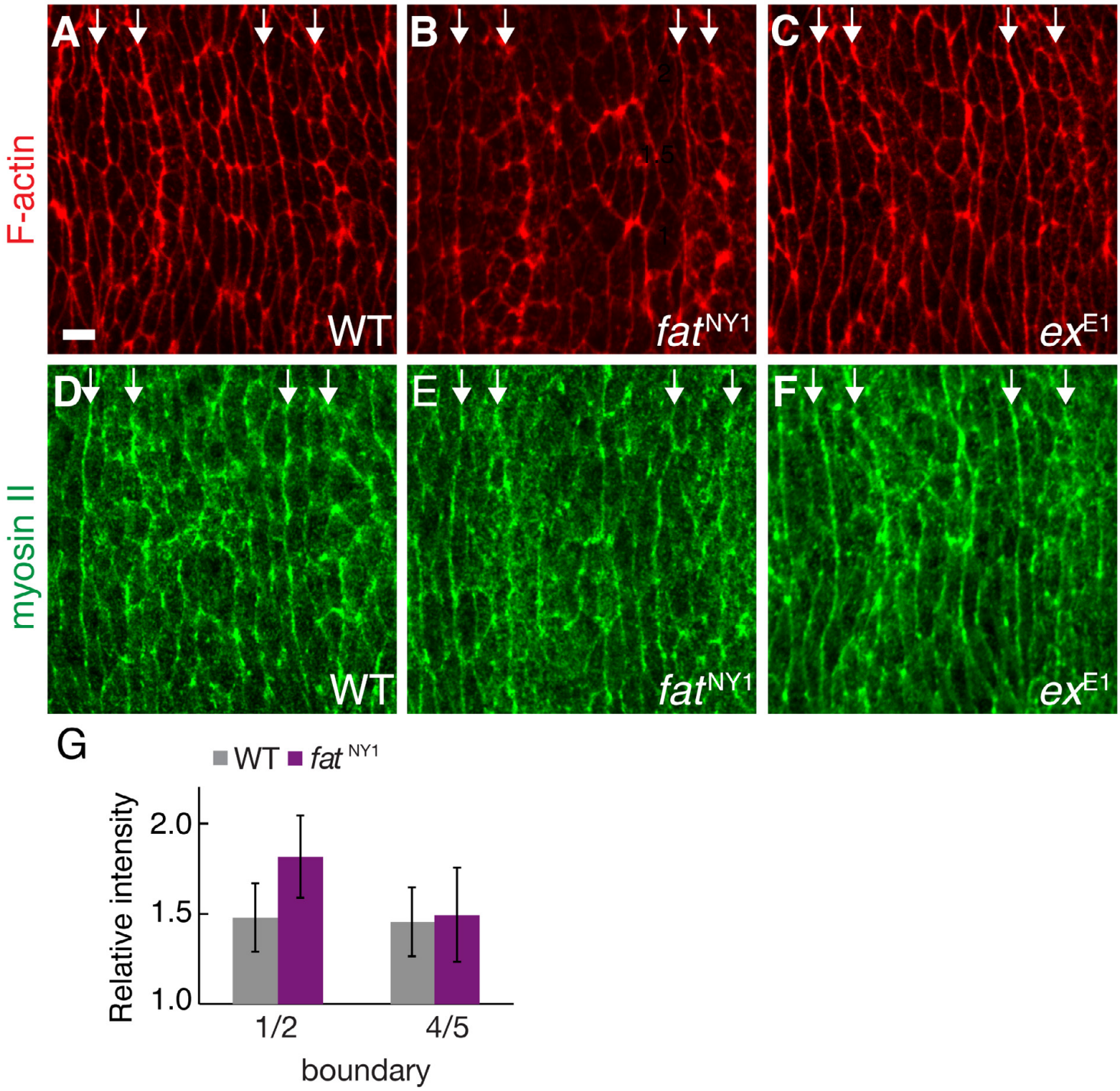

Fig. S3. Myosin and F-actin are correctly enriched at specific column boundaries in *fat* mutants. (**A-C**) Mid-stage 13 denticle belts in wild type (WT) (A), *fat*^{NY1} (B) and *ex*^{E1} (C) embryos stained with phalloidin to visualize F-actin. (**D-F**) Mid-stage 13 denticle belts in WT (D), *fat*^{NY1} (E) and *ex*^{E1} (F) embryos expressing a myosin II regulatory light chain GFP fusion (sqh:GFP) visualized with antibodies to GFP. Myosin II and F-actin accumulate at the column 1/2 and 4/5 boundaries (arrows) to a similar extent in WT, *fat* and *ex*. Ventral views, anterior left. (**G**) Enrichment of myosin II at AP edges compared with DV edges at the column 1/2 and 4/5 boundaries in WT and *fat*^{NY1}. In WT, myosin was enriched 1.5±0.2-fold at the column 1/2 boundary and 1.5±0.2-fold at the column 4/5 boundary. In *fat*^{NY1}, myosin was enriched 1.8±0.2-fold at the column 1/2 boundary and 1.5±0.3-fold at the column 4/5 boundary. A single value was obtained for each embryo by averaging the ratio of the average AP intensity to the average DV intensity for six to seven cells in two denticle belts/embryo (three to four embryos/genotype). The mean±s.e.m. of these values is shown. Scale bar: 5 μm.

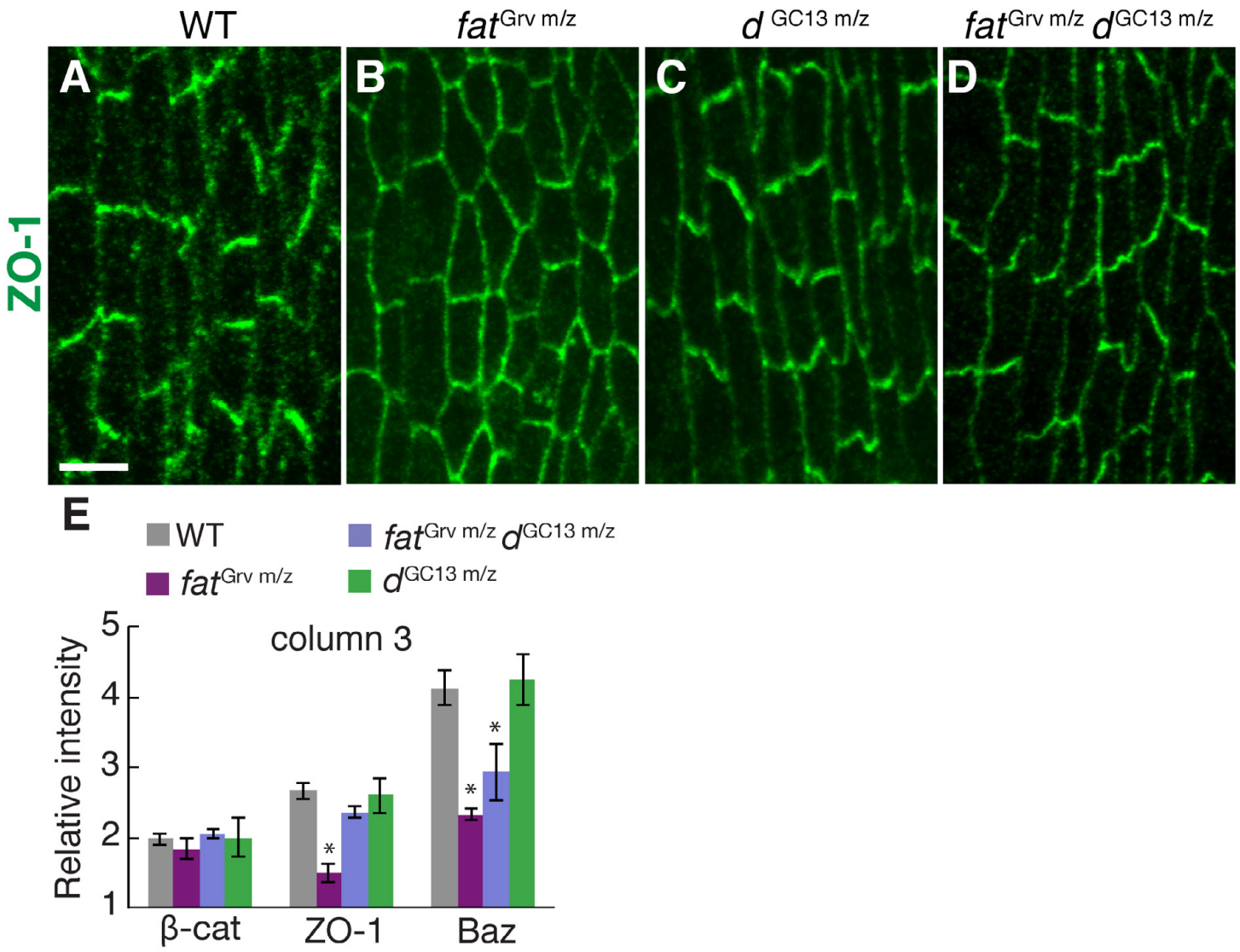

Fig. S4. Loss of *dachs* suppresses a subset of the junctional defects in *fat* mutants. (**A-D**) Stage 14 denticle belts stained for ZO-1 (green) in wild type (WT) (A) and embryos maternally and zygotically mutant for $fat^{Grv\ m/z}$ (B), $d^{GC13\ m/z}$ (C) and both $fat^{Grv\ m/z}$ and $d^{GC13\ m/z}$ (D). Scale bar: 5 μm. (**E**) Enrichment of junctional proteins at DV edges in column 3 of stage 14 embryos of the indicated genotypes. The enrichment of ZO-1 and Baz was significantly reduced in $fat^{Grv\ m/z}$ ($P<0.001$ for ZO-1 and $P<0.02$ for Baz). $d^{GC13\ m/z}$ was not significantly different from WT. Embryos doubly mutant for *fat* and *dachs* had WT ZO-1 localization ($P=0.2$ compared with WT, $P=0.04$ compared with $fat^{Grv\ m/z}$). However, Baz enrichment was significantly reduced in *fat dachs* double mutants ($P=0.02$ compared with WT), indicating that *dachs* does not suppress all aspects of the *fat* mutant phenotype. A single value was calculated for each embryo by measuring the ratio of average DV intensity to average AP intensity for five to seven cells in two denticle belts/embryo; $n=4$ embryos for each genotype. The mean±s.e.m. of these values is shown.

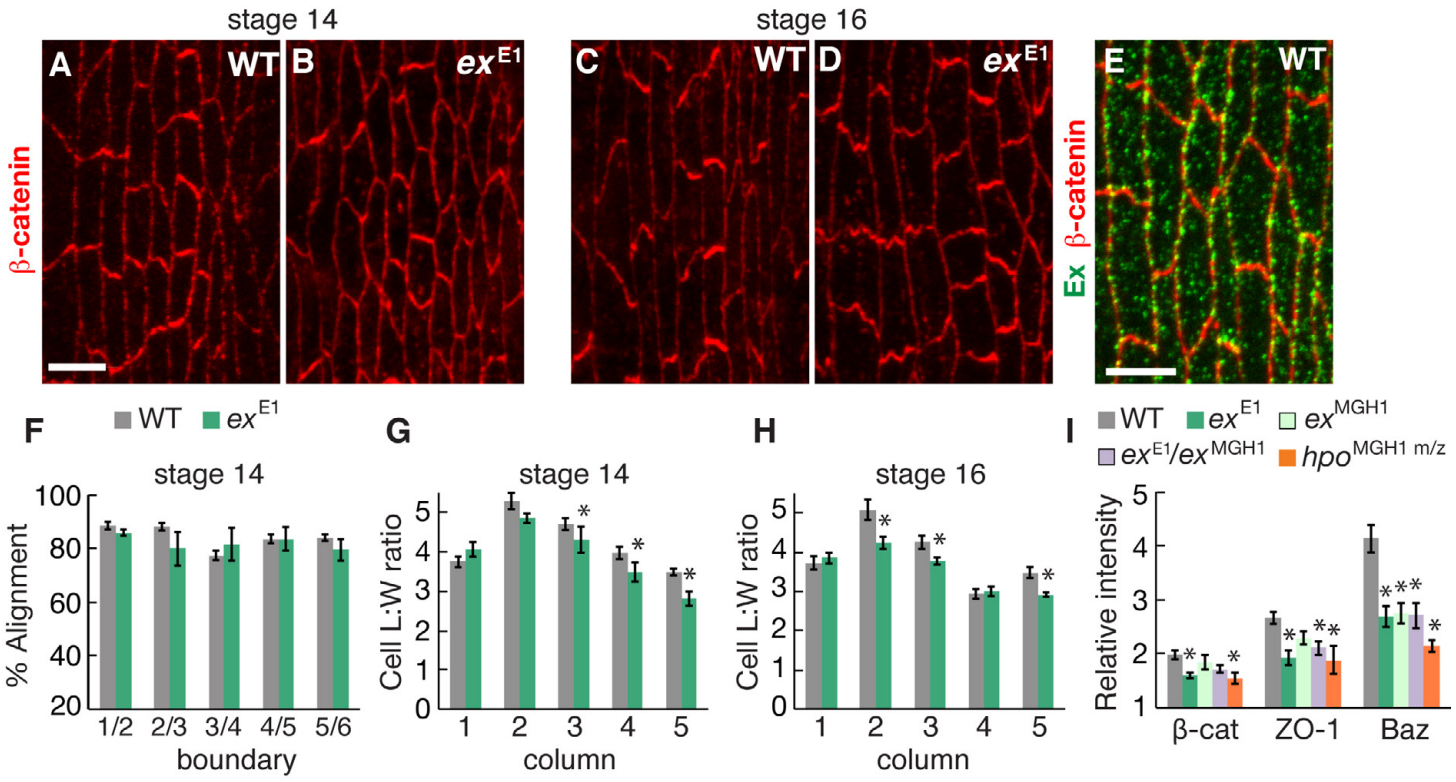

Fig. S5. Cell-shape defects in *expanded* mutants. (**A-D**) Denticle belts stained for β-catenin in wild type (WT) (A,C) and ex^{E1} (B,D) embryos at stage 14 (A,B) or stage 16 (C,D). Ventral views, anterior left. Scale bar: 5 μm. (**E**) WT denticle belt stained for Ex (green) and β-catenin (red) at stage 14. (**F**) Edge alignment in WT (gray) and ex^{E1} (green) at stage 14. Alignment in ex^{E1} was not significantly different from WT. A single value was obtained for each column boundary in each embryo by averaging all angles measured for that boundary (40 angles in four embryos/boundary). The mean±s.e.m. of these values is shown. (**G**,**H**) Cell length:width (L:W) ratios (the ratio of cell length along the DV axis to cell width along the AP axis) plotted by column in WT and ex^{E1} at stage 14 (G) and stage 16 (H). Cell L:W ratios were decreased in stage 14 ex^{E1} embryos compared with WT in columns 3 (P=0.02), 4 (P=0.04) and 5 (P<0.001), and in stage 16 ex^{E1} embryos in columns 2 (P=0.006), 3 (P=0.01) and 5 (P<0.001). A ratio was measured for each cell (30-75 cells in four embryos/column). The mean±s.e.m. of these values is shown. (**I**) Enrichment of junctional proteins at DV edges in column 3 of stage 14 WT, ex^{E1}, ex^{MGH1}, ex^{E1}/ex^{MGH1} and $hpo^{MGH1\ m/z}$ embryos. The enrichment of several junctional proteins at DV edges was significantly reduced in ex^{E1} (P<0.001 for β-catenin, ZO-1 and Baz), ex^{MGH1} (P=0.005 for Baz), ex^{E1}/ex^{MGH1} (P=0.04 for ZO-1; P=0.02 for Baz) and $hpo^{MGH1\ m/z}$ (P<0.02 for β-cat; P=0.006 for ZO-1; and P<0.001 for Baz). A single value was calculated for each embryo by measuring the ratio of the average DV intensity to the average AP intensity for five to seven cells in two denticle belts/embryo; n=4 embryos for each genotype. The mean±s.e.m. of these values is shown. Maternal gene products may obscure additional requirements for Ex, as we were unable to obtain embryos that lack maternal *ex* activity.

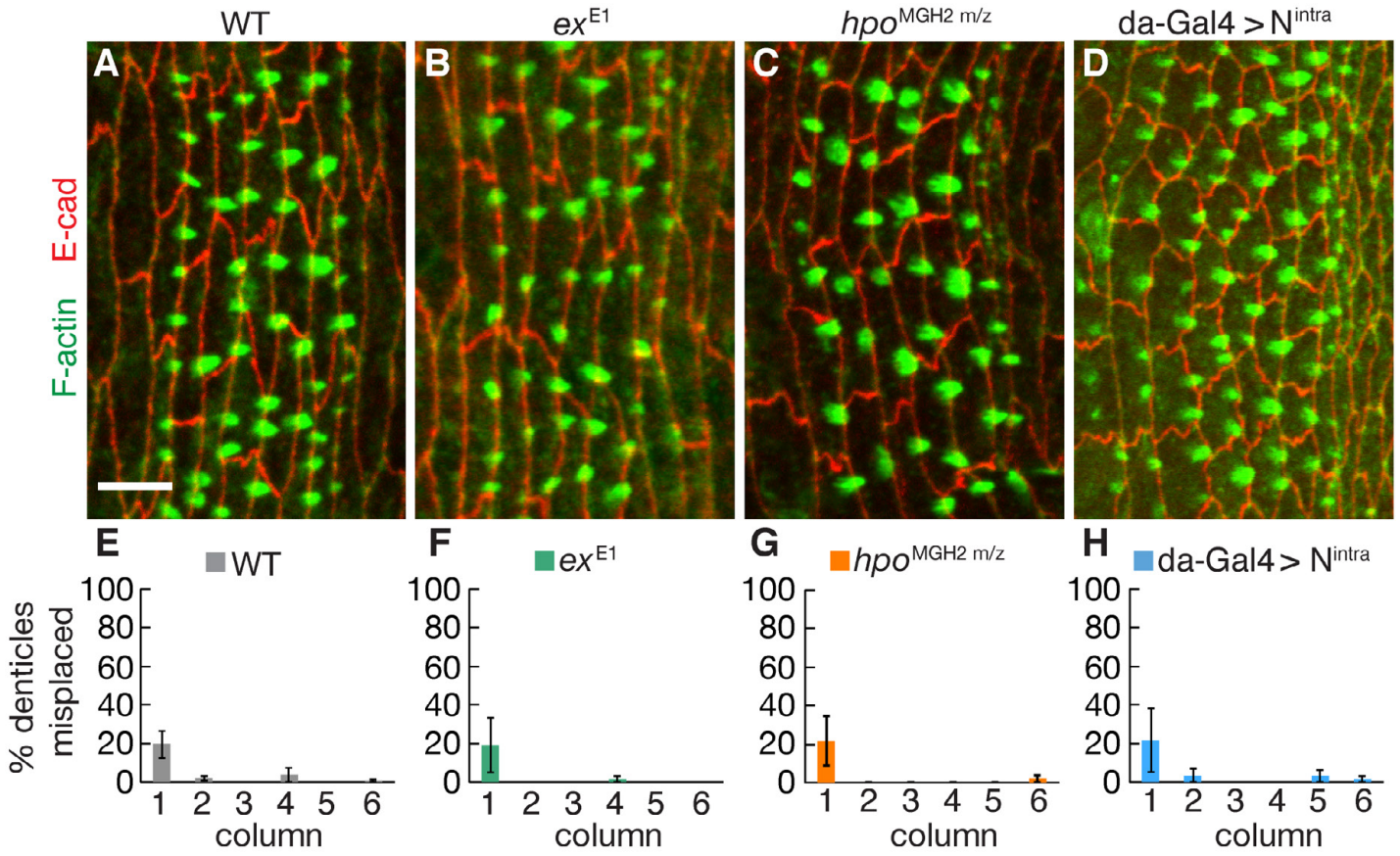

Fig. S6. Denticle placement in wild-type, *ex* mutant and N^{intra}-expressing embryos. (**A-D**) Stage 15 denticle belts stained for F-actin (phalloidin, green) and E-cadherin (red) in wild type (WT) (A), *ex*^{E1} (B), *hpo*$^{MGH2\ m/z}$ (C) and da-Gal4>N^{intra} (D) embryos. Scale bar: 5 μm. (**E-H**) Percentage of misplaced denticle precursors plotted by column for WT (E), *ex*^{E1} (F), *hpo*$^{MGH2\ m/z}$ (G) and da-Gal4>N^{intra} (H) embryos. Denticle precursors were correctly localized to the posterior cell cortex. Ventral views, anterior left. A single value was obtained for each column in each embryo (354-464 denticles in three to five embryos/genotype). The mean±s.e.m. of these values is shown.

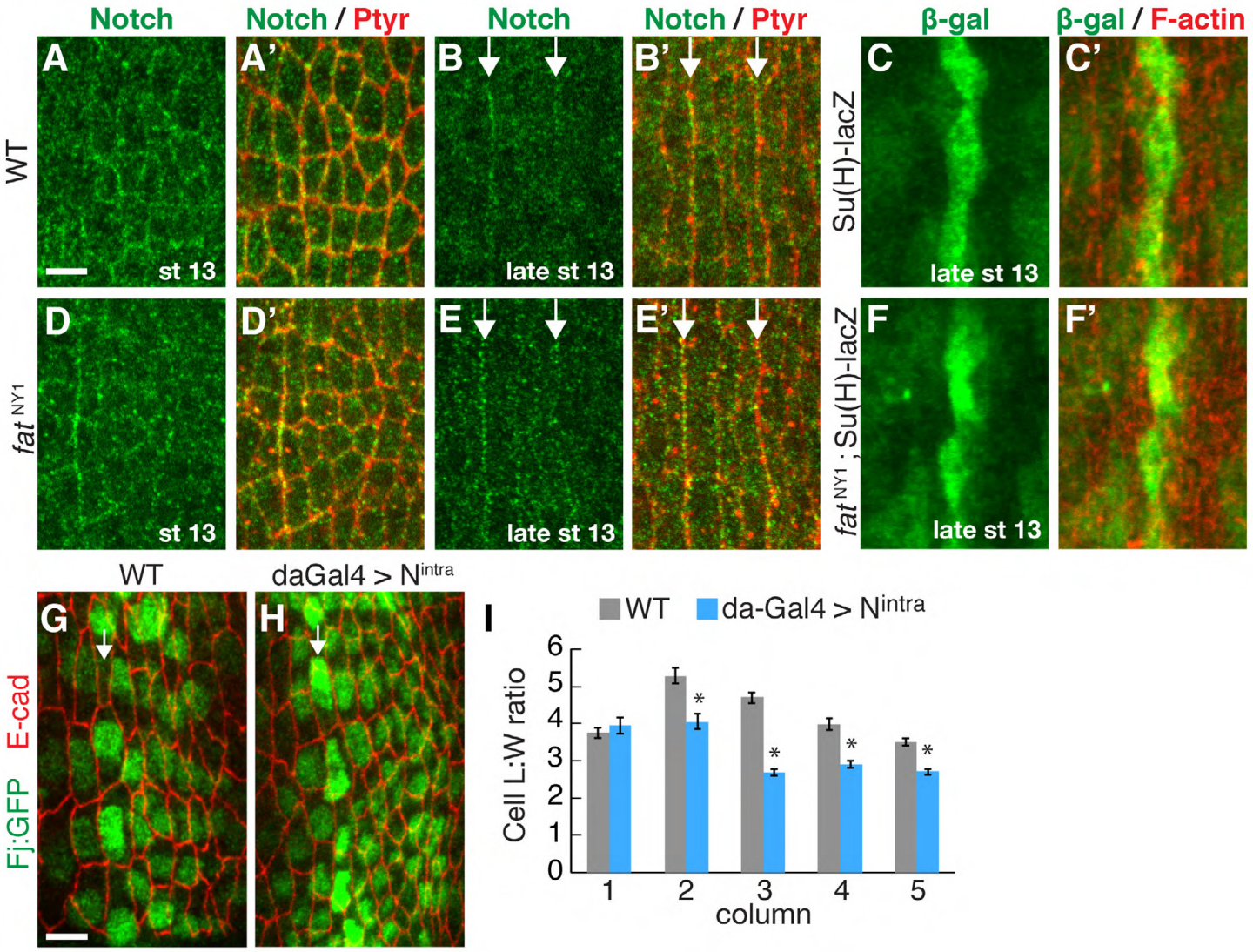

Fig. S7. Notch activation recapitulates the cell-shape defects of *fat* mutants. (**A-B′**,**D-E′**) Denticle belts at the indicated stages stained for Notch (green) and phosphotyrosine (Ptyr, red). (A,D) In early stage 13, Notch localizes to the apical cortex of wild-type (WT) (A) and *fat*^{NY1} (D) embryos. (B) In late stage 13, Notch is enriched at the column 1/2 and 4/5 boundaries (arrows) in WT. (E) This localization occurs normally in *fat*^{NY1}. (**C**,**F**) Late stage 13 denticle belts stained for F-actin (phalloidin, red) and β-gal (green) to visualize the expression of the Su(H)*lacZ* Notch activity reporter in WT (C) and *fat*^{NY1} (F). The column 4-specific pattern of Su(H)*lacZ* expression occurs normally in *fat*^{NY1}. Ventral views, anterior left. (**G**,**H**) Localization of the endogenous Four-jointed protein using a Four-jointed:GFP (Fj:GFP) trap line visualized with antibodies to GFP. Fj:GFP was expressed throughout the denticle field, with an enrichment in column 2 (arrows). This enrichment of Fj:GFP expression was retained in N^{intra}-expressing embryos, although a broadening of the Fj domain is apparent. (**I**) Cell length:width (L:W) ratios (the ratio of cell length along the DV axis to cell width along the AP axis) plotted by column in stage 14 WT and da-Gal4>N^{intra} embryos. Cell L:W ratios were decreased in da-Gal4>N^{intra} compared with WT in columns 2-5 (P<0.001). A ratio was measured for each cell (40-100 cells in four embryos/column). The mean±s.e.m. of these values is shown. Scale bars: 5 μm.